ISSN 0208-7774 T R I B O L O G I A 6/2019 p. 39–46
DOI: 10.5604/01.3001.0013.7765

Monika MADEJ*, Katarzyna PIOTROWSKA, Dariusz OZIMINA*****

PROPERTIES OF DIAMOND-LIKE CARBON COATINGS ON THE TITANIUM ALLOY Ti13Nb13Zr

WŁAŚCIWOŚCI POWŁOK DIAMENTOPODOBNYCH NA STOPIE TYTANU Ti13Nb13Zr

Key words: diamond-like carbon coating, titanium alloys, surface texture, friction, hardness, wear.

Abstract The paper discusses the results of experimental research on DLC type diamond coating a-C:H obtained by the technique of physical vapour deposition from PVD on titanium alloy Ti13Nb13Zr. Calotest and an optical microscope were used to determine the thickness of the obtained coating. The nano-hardness of uncoated and with a-C:H coating was determined by the indentation method using a Berkovich indenter. The geometric structure of the surface before and after tribological tests was assessed using a confocal microscope with an interferometric mode. Tests of the resistance of test materials to tribological wear were performed on a tribometer in reciprocating motion under technically dry friction, and friction with lubrication with an artificial blood solution and Ringer's solution. Tests carried out for the combination of a 6 mm diameter Al_2O_3 ball-Ti13Nb13Zr titanium alloy disc without and with the DLC coating applied. The results obtained during the tests showed that the use of the DLC coating increases the hardness five times and reduces the friction. In the case of technically dry friction, the coefficient of friction decreased by 70%, the solution of artificial blood by 50%, and in the case of Ringer's solution by 90%, in comparison with the results obtained for the Ti13Nb13Zr alloy.

Słowa kluczowe: powłoka diamentopodobna, stopy tytanu, struktura geometryczna powierzchni, tarcie, twardość, zużycie.

Streszczenie W pracy omówiono wyniki eksperymentalnych badań powłoki diamentopodobnej DLC typu a-C:H otrzymywanej techniką fizycznego osadzania z fazy gazowej PVD na stopie tytanu Ti13Nb13Zr. Do określenia grubości otrzymanych powłoki posłużył kulotester oraz mikroskop optyczny. Nanotwardość elementów bez powłoki oraz z powłoką a-C:H wyznaczono metodą indentacyjną przy użyciu wgłębnika Berkovicha. Strukturę geometryczną powierzchni przed i po testach tribologicznych oceniano za pomocą mikroskopu konfokalnego z trybem interferometrycznym. Badania odporności materiałów testowych na zużycie tribologiczne przeprowadzono na tribometrze w ruchu posuwisto-zwrotnym w warunkach tarcia technicznie suchego oraz tarcia ze smarowaniem roztworem sztucznej krwi i roztworem Ringera. Obecność płynu miała na celu symulowanie naturalnych warunków tribologicznych występujących w ciele człowieka. Testy zrealizowano dla skojarzenia: kulka z Al_2O_3 – tarcza ze stopu tytanu Ti13Nb13Zr bez oraz z naniesioną powłoką DLC. Otrzymane wyniki badań wskazały, że zastosowanie powłoki DLC spowodowało 5-krotne zwiększenie twardości oraz zmniejszenie oporów ruchu par trących we wszystkich zastosowanych warunkach tarcia. W przypadku tarcia technicznie suchego wartość współczynnika tarcia zmniejszyła się o 70%, roztworu sztucznej krwi o 50%, a w przypadku roztworu Ringera o 90% w porównaniu z wynikami uzyskanymi dla stopu Ti13Nb13Zr. Wyniki uzyskane podczas badań stanowią źródło wiedzy na temat stopu Ti13Nb13Zr, powłok diamentopodobnych oraz ich potencjalnego zastosowania w systemach biotribologicznych.

* ORCID: 0000-0001-9892-9181. Kielce University of Technology, Faculty of Mechatronics and Mechanical Engineering, Tysiąclecia Państwa Polskiego 7 Ave., 25-314 Kielce, Poland.
** ORCID: 0000-0001-6366-2755. Kielce University of Technology, Faculty of Mechatronics and Mechanical Engineering, Tysiąclecia Państwa Polskiego 7 Ave., 25-314 Kielce, Poland.
*** ORCID: 0000-0001-5099-6342. Kielce University of Technology, Faculty of Mechatronics and Mechanical Engineering, Tysiąclecia Państwa Polskiego 7 Ave., 25-314 Kielce, Poland.

INTRODUCTION

Modern industry places high demands on materials concerning mechanical, tribological, and anti-corrosive properties. For many years, research has been carried out to improve the materials used today, both in terms of components and design. In addition, increasing the service life of materials is possible due to the use of surface engineering methods, including physicochemical treatments and the formation of surface layers and coatings. For example, diamond-like coatings combining the properties of a diamond – thanks to the content of sp^3-type bonds, a high hardness is obtained, and graphite – containing sp^2 bonds, resulting in excellent lubricating properties. Diamond-like DLC carbon coatings are a mixture of amorphous or fine crystalline carbon with a hybridization of the already mentioned sp^2 and sp^3 as well as sp^1 **[L. 1–3]**. At present, diamond coatings are understood to mean amorphous, in most cases, hydrogenated thin-film materials with different properties, depending on the type of method used and the conditions under which they are deposited.

The DLC diamond coatings are characterized by very good mechanical parameters: high modulus of elasticity, resistance to brittle cracking and chemical stability. Having these features allows them to be used in tribological systems where a low friction coefficient and high resistance to wear and tear is required, e.g., in the automotive and aerospace industries, and in medicine **[L. 4]**. The disadvantage of diamond-like coatings is that they have high internal stresses, which may reduce the adhesion of the coating to the substrate. To prevent this, the coating is either mixed with other elements or interlayers are used during the application process. The application of the interlayer allows one to reduce stresses and maintain high operational parameters **[L. 5–8]**.

Chemical (CVD) and physical vapour deposition (PVD) methods are used to produce thin, diamond-like coatings. The CVD methods require the use of high temperatures necessary for the decomposition of gas reagents (of the order of 900–1100°C or even higher) and for the course of chemical reactions – enabling the formation of coatings, which significantly limits the scope of their use. In the CVD method, a layer of new material is formed on the surface of the heated substrate as a result of chemical reactions occurring in the gas or vapour phase **[L. 9–10]**. Currently, there are several dozen known varieties and modifications of the PVD methods, the common feature of which is the use of various physical phenomena taking place at reduced pressure in the range of $10 – 10^{-5}$ Pa. In the PVD physical vapour deposition method, thin layers are formed as a result of condensation of metal atoms or ions released from the solid or liquid in physical processes through evaporation or spraying **[L. 11–14]**. In almost all PVD methods, the coating deposited on the substrate is formed by a flux of ionized plasma directed electrically to a relatively cold substrate (200–600°C), which allows the substrate to be covered without fear of a decrease in its initial hardness. The connection between the coating and the substrate is adhesive (less frequently adhesive-diffusive) in nature and becomes weaker, the less clean the covered surface is **[L. 9, 15]**.

The operational and functional properties of the created layers depend on the chemical composition, metallographic structure, and adhesion of the coating to the substrate. Chemical composition, structure, and adhesion depend on the type and mutual ratio of the substrates. The type of method and the technical and technological parameters of the application determine the operational properties of the coatings. Usually, the same coatings deposited by different methods exhibit different performance characteristics **[L. 16]**. In both the PVD and the CVD methods, plasma-aided lowering of the temperature of the process is possible.

Application of modern techniques of coating manufacture allows one to obtain surfaces with better mechanical and tribological properties, which translates into longer working time of tribological systems and increased operational durability.

The aim of this study was to evaluate the geometric structure of the surface, the tribological properties, and the hardness of DLC coating of the a-C:H type deposited via the PVD method on Ti13Nb13Zr titanium alloy.

MATERIALS AND METHODS

Single-layer diamond coating of the a-C:H type were applied via PVD physical deposition from the gas phase at temperatures below 250ºC. The substrate was the Ti13Nb13Zr titanium alloy, and the elemental composition is presented in **Table 1.**

Table 1. Chemical composition of titanium and its alloy, % wag
Tabela 1. Skład chemiczny tytanu i jego stopów w % wag

Element	% weight							
	C	H	O	N	Fe	Nb	Zr	Ti
Ti13Nb13Zr	≤ 0.08	≤ 0.015	≤ 0.016	≤ 0.05	≤ 0.25	12.5–14.0	12.5–14.0	based

Optical microscopy was used to observe the samples with DLC coating applied. The studies included observations of surface topography of samples before and after tribological tests.

The coating thickness was measured using an Anton Paar's CatC Calotester and an optical microscope. Thickness was measured by abrading the coating with a ball, 20 mm in diameter, moving at 620 rpm. A drop of polishing suspension (0 – 0.2 µm gradation) was applied in place of contact between the sample and the ball. A diagram of the friction pair is shown in **Fig. 1**.

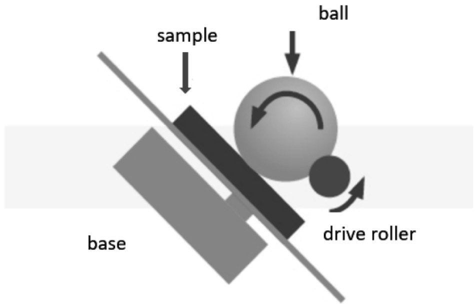

Fig. 1. Friction pair
Rys. 1. Schemat węzła tarcia

The hardness was determined using the UNHT ultra-nano hardness tester from Anton Paar using the instrumental indentation method. Olivier Pharr's method was used to determine the nano-hardness. The measurement was made at a nominal load force of 100 mN and a build up speed of 200 mN/min. The test consisted in pushing a penetrator of known geometry into the tested material, simultaneously recording the load and penetration depth. A diamond penetrator with Berkovich geometry with a radius of tip rounding of R_i = 100 nm was used for the measurement. The geometry of the penetrator used is shown in **Fig. 2**.

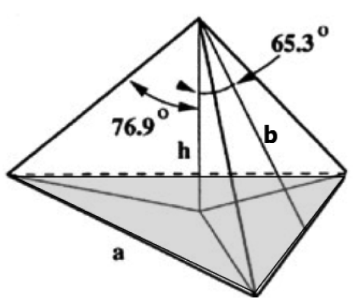

Fig. 2. Geometry of Berkovich indenter
Rys. 2. Geometria wgłębnika Berkovicha

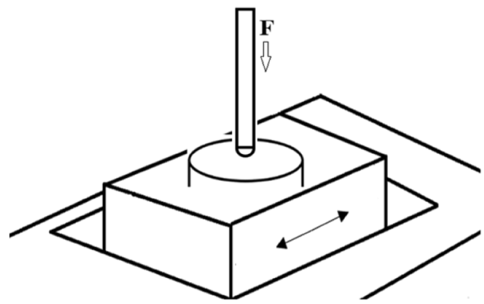

Fig. 3. View of ball-on-disc
Rys. 3. Widok węzła tarcia

Tribological tests were carried out on the TRB[3] ball-on-disc tribometer in reciprocal motion. The view of the friction pair is shown in **Fig. 3.** The tribological tests were carried out with the technical and environmental parameters presented in **Table 2**. Balls made of aluminium oxide (III) – Al_2O_3 with a diameter of 6 mm *(Ra* 0.37 µm) were used as the counter-sample in the friction pairs.

Table 2. Technical and environmental parameters of test
Tabela 2. Parametry techniczne i środowiskowe testu

Parameter	Unit	Friction pair
		ball Al_2O_3 – disc Ti13Nb13Zr ball Al_2O_3 – disc Ti13Nb13Zr with a-C:H coating
Load	N	5
Linear speed	m/s	0.0159
Cycle	–	10 000
Frequency	Hz	1
Humidity	%	50 ± 1
Temperature	˚C	23±1
Lubricant	–	Without Artificial blood Ringer solution

The tribological tests were repeated 5 times for each friction pair at the set parameters. The chemical compositions of the lubricants used are shown in **Tables 3 and 4**. The presence of the solutions was intended to create conditions similar to the natural tribological conditions present in a human body. During the tests, a 1.5 ml of the solution was applied on the sample with a pipette.

Table 3. Chemical composition of artificial blood (AB)
Tabela 3. Skład chemiczny roztworu sztucznej krwi

Chemical composition [g/dm³]								
NaCl	$NaHCO_3$	KCl	K_2HPO_4*$3H_2O$	$MgCl_2$*$6H_2O$	$CaCl_2$	Na_2SO_4	$(CH_2OH_3)_3CNH_2$	1 mol HCl
7.996	0.350	0.224	0.228	0.305	0.278	0.071	6.057	1.46

Table 4. **Chemical composition of Ringer solution (RS)**
Tabela 4. Skład chemiczny roztworu Ringera

Chemical composition [g/dm³]		
NaCl	KCl	$CaCl_2$
8.6	0.3	0.243

RESULTS

The thickness of the diamond-like coating was measured at 1.92 µm using a Calotester and an optical microscope. **Figure 4** shows the wear trace.

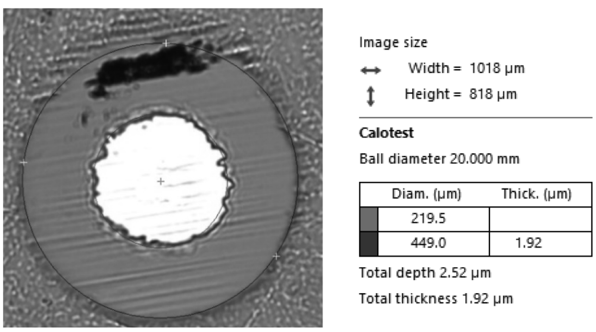

Fig. 4. **Thickness of DLC carbon coating**
Rys. 4. Pomiar grubości powłoki diamentopodobnej

UNHT ultra-nano hardness tester was used to evaluate the mechanical properties – nanohardness of the coating. The operating parameters of the device during the tests are listed in **Table 5.**

Table 5. **Technical parameters of mechanical measurements**
Tabela 5. Parametry techniczne pomiarów mechanicznych

Parameter	Unit	Value
Acquisition rate	Hz	10
Max. load	nM	100
Loading rate	Hz	200
Unloading rate	mN/min	200
Pause	s	5
Linear Loading		

Figures 5a and 5b show the load curves – the load relief recorded when the indenter is pushed into the tested materials. Hardness and Young's modulus based on Olivier Pharr's methodology were determined on the basis of measurements of the penetrator's penetration depth and knowledge of imprint geometry. **Table 6** presents averaged values of selected mechanical parameters obtained from 10 measurements.

a)

b)

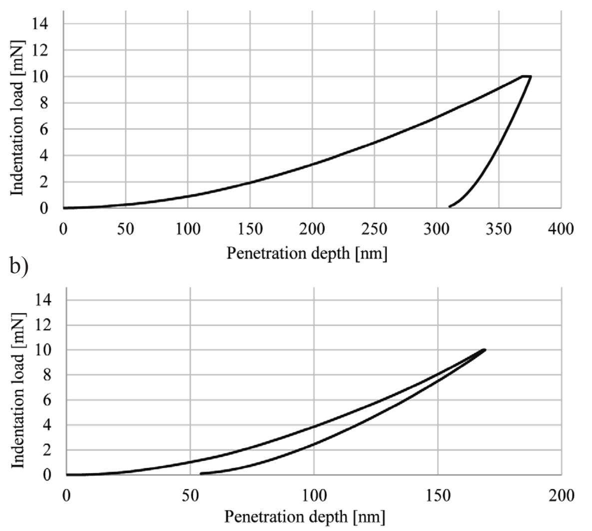

Fig. 5. **Load – penetration depth curves from indentation tests for a) Ti13Nb13Zr, b) Ti13Nb13Zr a-C: H**
Rys. 5. Krzywe zależności siły od głębokości penetracji wgłębnika dla a) Ti13Nb13Zr, b) Ti13Nb13Zr a-C:H

Table 6. **Characteristics of mechanical properties**
Tabela 6. Charakterystyka własności mechanicznych

Parameter	Unit	Sample	
		Ti13Nb13Zr	Ti13Nb13Zr a-C:H
Instrumental Hardness [H_{IT}]	GPa	3	19
Vickers Hardness [HV]	HV	346	1807
Young Modulus [E^*]	GPa	118	176
Contact area [A_p]	nm^2	34514832	514247
Plastic work [W_{plast}]	pJ	32417	182
Elastic work [W_{elast}]	pJ	7622	479

The curves shown in **Fig. 5** indicate the high elasticity of the a-C:H coating and the plasticity of the substrate. This is evidenced by the slope of the indentation curve and the values of plastic and elastic work obtained (**Table 6**). As a result of application of the diamond-like coating, the instrumental hardness and Vickers hardness increased by five times. Moreover, for the a-C:H coating, an increase in Young's modulus of about 35% was also observed in comparison with the values obtained for the Ti13Nb13Zr alloy.

Figure 6 shows the results of measurements of the geometric structure of the surface prior to the tribological tests. On both surfaces, a similar value of the *Ra* parameter (arithmetic mean of roughness profile deviation) was recorded. For Ti13Nb13Zr it was 7.95 nm, and 10.32 nm for the diamond-like coating. On the other hand, observations of the surface profile unequivocally indicate indentations and elevations of up

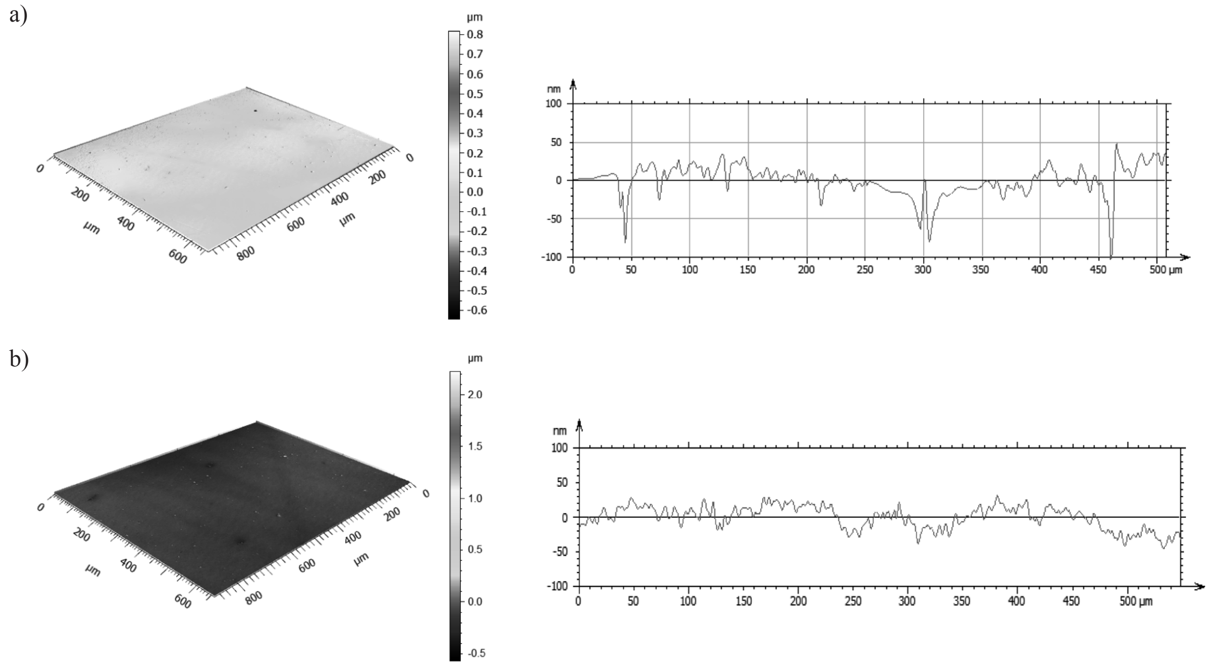

Fig. 6. The isometric image of surface and the profile of surface: a) Ti13Nb13Zr, b) Ti13Nb13Zr a-C:H

Rys. 6. Obrazy izometryczne i profile powierzchni Ti13Nb13Zr, b) Ti13Nb13Zr a-C:H

to 50 nm in the case of the substrate itself. The surface profile recorded for the DLC coating is characterized by indentations and elevations half the size of the substrate. This indicates a more even surface topography after the a-C:H coating has been deposited, because both indentations and elevations have been levelled.

In order to evaluate the tribological properties of the tested materials, friction tests were performed. The results obtained were summarized on a graph of the friction coefficient – μ (**Fig. 7**) – of test elements depending on the types of materials, friction pairs,

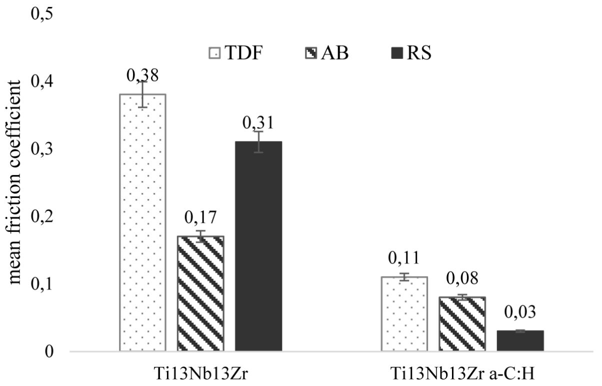

Fig. 7. Mean coefficient of friction during: technical dry friction (TDF), artificial blood (AB) and Ringer solution (RS)

Rys. 7. Średnie współczynniki tarcia podczas: tarcia technicznie suchego (TDF), tarcia ze smarowaniem roztworem sztucznej krwi (AB) oraz roztworem Ringera (RS)

and lubricants used. The graph shows that the best tribological characteristics were obtained for the material combination of Ti13Nb13Zr with a DLC Al_2O_3 coating regardless of the test conditions (technically dry friction, friction with lubrication with artificial blood solution and Ringer's solution).

After the tribological tests, the samples were subjected to wear and tear measurements **(Figs. 8–11**). **Figures 8–9** show isometric images and abrasion profiles of the tested discs. The maximum depth **(Fig. 10**) and the wear area **(Fig. 11**) on the cross-section were assumed as the measure of wear.

The analysis of the geometric structure of the surface showed that, in all the friction pairs, there was a uniform surface wear of the top layer. In addition, the optical profilometric wear measurements showed that the Ti13Nb13Zr alloy sample with the diamond-like coating of type a-C:H was practically free from the wear resulting from tribological tests. The largest abrasion area was observed for the tests carried out under technically dry friction conditions. It was about 65% higher than the values recorded for friction under conditions of lubrication with artificial blood solution and Ringer's solution. For an uncoated sample, the highest wear was recorded for tests using the artificial blood solution. It was about 20% higher in comparison with the results obtained for other test conditions (TDF, RS). Moreover, in the case of the sample made of the Ti13Nb13Zr alloy, there was a characteristic accumulation of the edges of the abrasion marks, which indicates a typically abrasive wear mechanism.

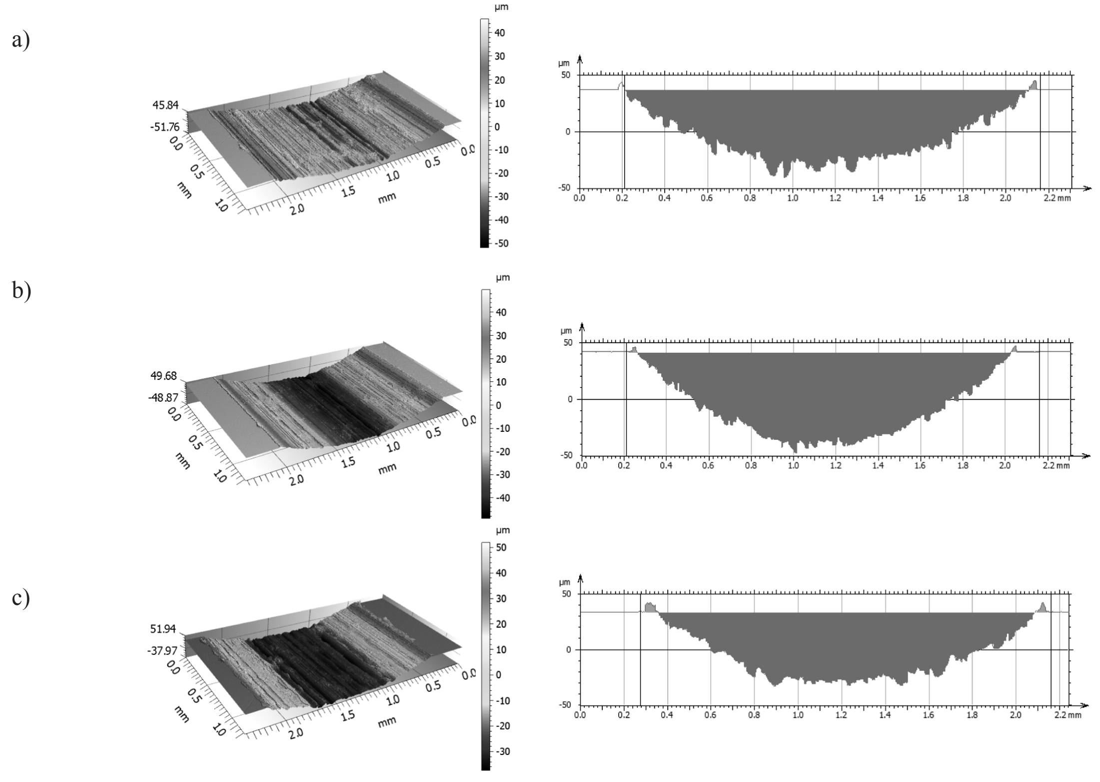

Fig. 8. The isometric image of the wear trace and the wear profile in a cross-section for Ti13Nb13Zr a) TDF, b) AB, c) RS

Rys. 8. Obrazy izometryczne i profile śladów wytarcia na przekroju poprzecznym dla stopu Ti13Nb13Zr podczas a) TDF, b) AB c) RS

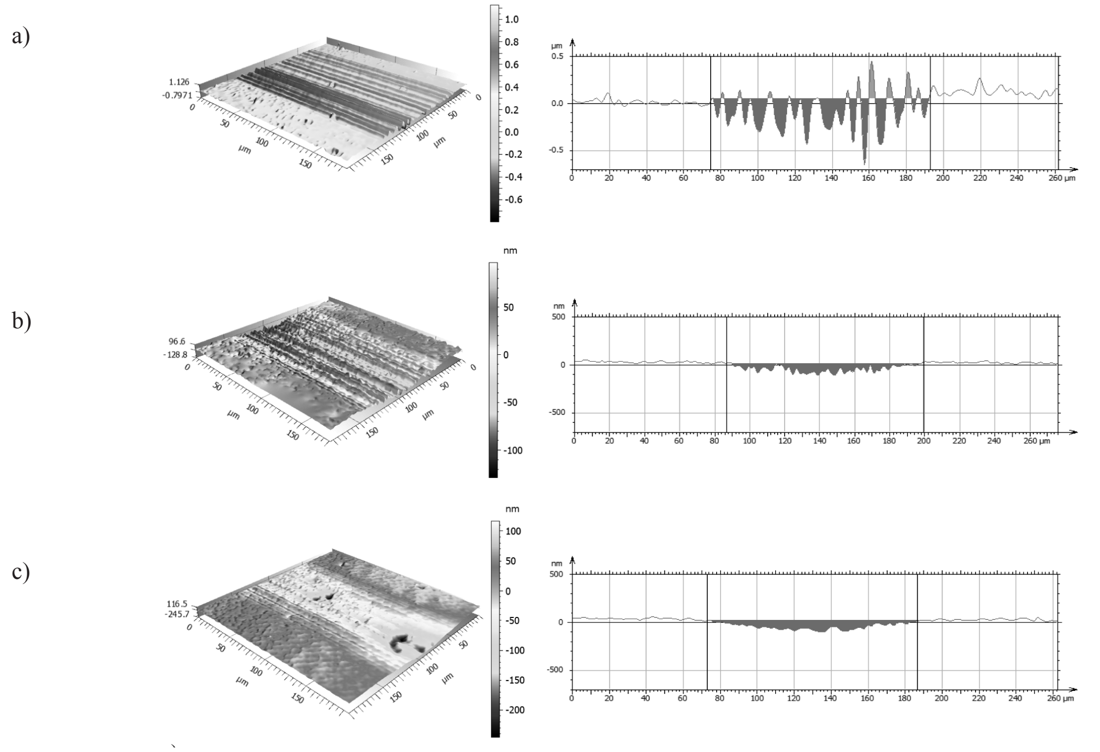

Fig. 9. The isometric image of the wear trace and the wear profile in a cross-section for Ti13Nb13Zr a-C:H a) TDF, b) AB, c) RS

Rys. 9. Obrazy izometryczne i profile śladów wytarcia na przekroju poprzecznym dla stopu Ti13Nb13Zr a-C:H podczas a) TDF, b) AB c) RS

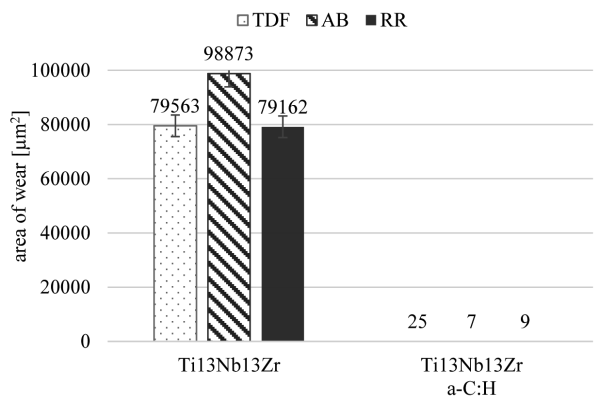

Fig. 10. Maximum depth of wear in a cross-section
Rys. 10. Maksymalna głębokość wytarcia na przekroju poprzecznym

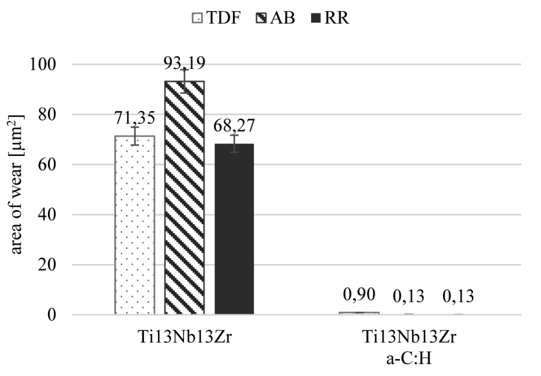

Fig. 11. The area of wear in a cross-section
Rys. 11. Pole powierzchni wytarcia na przekroju poprzecznym

CONCLUSIONS

The coating thickness tests carried out for this paper indicate that the thickness of the coating is 1.92 µm. The nano-hardness results draw attention to the different behaviour of the substrate and coating. The slope character of the indentation curves shows that the a-C:H coating is highly elastic and the substrate is plastic. As a result of application of the diamond-like coating, a increase of the hardness of 500% was achieved. Moreover, there was also a 35% increase in Young's modulus compared to Ti13Nb13Zr. The best tribological characteristics were obtained for the material combination Ti13Nb13Zr a-C:H – Al2O3 both during in the conditions: TDF, AB, and RS. The friction coefficients recorded were 70%, 50%, and 90% lower, respectively, compared to the values obtained for the substrate. Test results of the geometric structure of the surface after tribological tests shows that the diamond-like coating has a high resistance to abrasion. This is evidenced by the very small area of the scratch field. The analysis of the traces of wear also allowed for the identification of the wear mechanism. The presence of a build-up of wear trace edges means that, for the Ti13Nb13Zr alloy, abrasive wear was dominant.

REFERENCES

1. Poręba M., Reichert M., Sieniawski J., Zawadzka P.: Ocena powłoki diamentopodobnej wytworzonej na podłożu nadstopu niklu IN718 w procesach CVD wspomaganych plazmą wyładowania jarzeniowego, inżynieria materiałowa, 4, 35, 2014.
2. Piotrowska K., Madej M., Baranowicz P., Wysokińska-Miszczuk J.: The influence of diamond-like coatings on the properties of titanium, Materials Research Proceedings, 2018.
3. Jastrzębski K., Jastrzębska A., Bociaga D.: A review of mechanical properties of Diamond-Like Carbon coatings with various dopants as candidates for biomedical applications, Acta Innovations, 2017.
4. Braceras I., Ibáñez I., Dominguez-Meister S., Velasco X., Brizuela M., Garmendia I.: Electro-tribological properties of diamond like carbon coatings, Friction, 2019.
5. Madej M., Ozimina D., Gałuszka R., Gałuszka G.: Corrosion, friction and wear performance of diamond like carbon coating, Metallurgija, 2016.
6. Michalczewski R., Kalbarczyk M., Mańkowska-Snopczyńska A., Wieczorek A.: The Effect of a Gear Oil on Abrasion, Scuffing, and Pitting of the DLC-Coated 18CrNiMo7-6 Steel, Coatings, 2018.
7. Derakhshandeh M.R., Eshraghi M.J., Javaheri M., Khamseh S.: Diamond-like Carbon-Deposited Films: A New Class of Bio-Corrosion Protective Coatings, Surface Innovations, 2018.
8. Kot M., Major Ł., Major R., Lackner J., Pontie M.: Coatings with advanced microstructure for biomedical applications, Tribologia, 2, 2017.
9. Czechowski K.: Effect of nanostructured multilayer coatings on functional properties of tools, Mechanik, 1, 2017.
10. Januś M.: DLC Layers Created Using CVD Techniques and Their Application, Chemical Vapor Deposition for Nanotechnology, 2018.

11. Avelar-Batista J.C., Spain E., Fuentes G.G. Sola A., Rodriguez R., Housden J.: Triode plasma nitriding and PVD coating: A successful pre-treatment combination to improve the wear resistance of DLC coatings on Ti6Al4V alloy, Surface and Coatings Technology, 2006.
12. Burakowski T., Wierzchoń T.: Inżynieria powierzchni metali – podstawy, urządzenia, technologie, 1995.
13. Baptista A., Silva F.J.G., Porteiro J., Míguez L., Pinto G., Fernandes L.: On the Physical Vapour Deposition (PVD): Evolution of Magnetron Sputtering Processes for Industrial Applications, Procedia Manufacturing, 17, 2018.
14. Kocemba W.: Powłoki PVD BALINIT, Wybrane zastosowania. Inżynieria Powierzchni, 2, 2005.
15. Burakowski T., Miernik K., Walkowicz J.: Technologie wytwarzania z wykorzystaniem plazmy cienkich powłok tribologicznych. Metaloznawstwo, Obróbka cieplna, Inżynieria powierzchni, pp. 124–126, 1993.
16. Posti E., Nieminen I.: Influence of coating thickness on the life of TiN – coated high speed steel cutting tools, Wear, 129, 1989.